

Dynamical Multiple-Timestepping Methods for Overcoming the Half-Period Time Step Barrier

Siu A. Chin

Department of Physics, Texas A&M University, College Station, TX 77843, USA

Current molecular dynamic simulations of biomolecules using multiple time steps to update the slowly changing force are hampered by an instability occurring at time step equal to half the period of the fastest vibrating mode. This has become a critical barrier preventing the long time simulation of biomolecular dynamics. Attempts to tame this instability by altering the slowly changing force and efforts to damp out this instability by Langevin dynamics do not address the fundamental cause of this instability. In this work, we trace the instability to the non-analytic character of the underlying spectrum and show that a correct splitting of the Hamiltonian, which render the spectrum analytic, restores stability. The resulting Hamiltonian dictates that in addition to updating the momentum due to the slowly changing force, one must also update the position with a modified mass. Thus multiple-timestepping must be done dynamically.

I. INTRODUCTION

The evolution of any dynamical variable $W(q_i, p_i)$ is given by the Poisson bracket,

$$\frac{d}{dt}W(q_i, p_i) = \{W, H\} \equiv \sum_i \left(\frac{\partial W}{\partial q_i} \frac{\partial H}{\partial p_i} - \frac{\partial W}{\partial p_i} \frac{\partial H}{\partial q_i} \right). \quad (1.1)$$

For the standard Hamiltonian,

$$H(p, q) = \sum_i \frac{p_i^2}{2m_i} + v(q_i), \quad (1.2)$$

the Poisson evolution equation (1.1) can be written as an operator equation

$$\frac{dW}{dt} = \sum_i \left(\frac{p_i}{m_i} \frac{\partial}{\partial q_i} + F_i \frac{\partial}{\partial p_i} \right) W, \quad (1.3)$$

with formal solution

$$W(t) = e^{t(T+V)} W(0) = \left[e^{\epsilon(T+V)} \right]^n W(0), \quad (1.4)$$

where T and V are first order differential operators defined by

$$T \equiv \sum_i \frac{p_i}{m_i} \frac{\partial}{\partial q_i}, \quad V \equiv \sum_i F_i \frac{\partial}{\partial p_i}. \quad (1.5)$$

Their exponentiations, $e^{\epsilon T}$ and $e^{\epsilon V}$, are then *displacement* operators which displace q_i and p_i forward in time via

$$q_i \rightarrow q_i + \epsilon \frac{p_i}{m_i} \quad \text{and} \quad p_i \rightarrow p_i + \epsilon F_i. \quad (1.6)$$

Each factorization of $e^{\epsilon(T+V)}$ into products of $e^{\epsilon T}$, $e^{\epsilon V}$ (and exponentials of commutators of T and V) give rises to a *symplectic* algorithm for evolving the system forward in time. This is the fundamental Lie-Poisson theory of symplectic integrators, which has been studied extensively in the literature^{1,2,3}. First and second order factorizationa of the form

$$e^{\epsilon(T+V)} \approx e^{\epsilon T} e^{\epsilon V} \quad (1.7)$$

$$\approx e^{\frac{1}{2}\epsilon V} e^{\epsilon T} e^{\frac{1}{2}\epsilon V} \quad (1.8)$$

give rises to the well-known symplectic Euler and the velocity-Verlet algorithm. Numerous higher order symplectic algorithms^{3,4,5,6,7,8} are also known, but only a special class of fourth order algorithms can have strictly positive time steps as these lower order algorithms^{9,10}.

In many cases, the Hamiltonian of interest is of the form,

$$H(p, q) = \frac{p^2}{2m} + v_1(q) + v_2(q), \quad (1.9)$$

where there is a “fast” force component $F_1 = -\partial_q v_1$ and a “slow” force component $F_2 = -\partial_q v_2$. For example, in biomolecular dynamics, F_1 can be the rapidly vibrating force of H-O bonds and F_2 , the sum of non-bond forces. Since it seems reasonable to sample the slowly changing force F_2 less frequently, one can factorize this Hamiltonian to first or second order,

$$e^{\Delta t(T+V_1+V_2)} = e^{\Delta t(T+V_1)} e^{\Delta t V_2}, \quad (1.10)$$

$$= e^{\frac{1}{2}\Delta t V_2} e^{\Delta t(T+V_1)} e^{\frac{1}{2}\Delta t V_2}, \quad (1.11)$$

and solve for the fast force accurately using a smaller time step $\Delta\tau = \Delta t/k$,

$$e^{\Delta t(T+V_1)} = \left[e^{\Delta\tau T} e^{\Delta\tau V_1} \right]^k, \quad (1.12)$$

$$= \left[e^{\frac{1}{2}\Delta\tau V_1} e^{\Delta\tau(T+V_1)} e^{\frac{1}{2}\Delta\tau V_1} \right]^k. \quad (1.13)$$

Thus the slow force is sampled at a multiple time steps of the fast force, $\Delta t = k\Delta\tau$. In the context of biomolecular simulation, this form of the multiple-time step (MTS) symplectic algorithm was introduced by Grubmüller *et al.*¹¹, and independently by Tuckerman *et al.*¹². If a large time step Δt can be used in MTS algorithms, one can hope to simulate the motion of macromolecules through some biologically significant time intervals.

In the subsequent work of Zhou and Berne¹³ and Watanabe and Karplus¹⁴, this hope was dashed by the discovery of an intransigent instability. No matter how accurately one has solved the fast force, the MTS algorithm is unstable at $\Delta t = \pi/\omega_1$, where ω_1 is the fast force’s vibrational angular frequency. This has been described as a “resonance” instability^{15,16,17}. However, the later numerical work of Barth and Schlick¹⁸ clearly demonstrates that this instability exists at every mid-period as well, *i.e.*, at $\Delta t = n\pi/\omega_1 = (n/2)T_1$, where T_1 is the period of the fast force, at $n = 1, 2, 3, \dots$, and not just at $n = 2, 4, 6, \dots$. Thus the notion of resonance is not a complete nor accurate description of this instability. In this work, we will show that this instability is fundamentally related to the non-analytic character of the harmonic spectrum and cannot be tamed by just multiple-timestepping the slow force. Stability can only be restored by a different splitting of the Hamiltonian requiring the slow force to be updated dynamically with a modified mass.

In the next section, we analyze Barth and Schlick’s model of MTS instability¹⁸ and show that *static* multiple-timestepping of the slow force destabilizes the marginally-stable points of the fast force. In Section III, we show that an alternative splitting of the Hamiltonian, that of *dynamic* multiple-timestepping of the slow force, restores stability. In Section IV, we explain why the particular splitting worked in terms of the analytic character of the resulting spectrum. Section V generalizes MTS to the case of multiple forces. Section VI summarizes our findings and suggestions for large scale biomolecular simulations.

II. STABILITY ANALYSIS OF MTS ALGORITHMS

Barth and Schlick¹⁸ have proposed the simplest and clearest model for understanding the MTS instability. This is a harmonic oscillator with two spring constants,

$$v_1(q) = \frac{1}{2}\lambda_1 q^2, \quad v_2(q) = \frac{1}{2}\lambda_2 q^2. \quad (2.1)$$

Their numerical work unambiguously demonstrated the existence of MTS instability, but they did not carry their analysis far enough to pinpoint its origin. We will first complete their analysis of the symplectic Euler MTS algorithm.

Each operator $e^{\Delta\tau T}$, $e^{\Delta\tau V_1}$, when acting on the canonical doublet (p, q) , produces a symplectic transformation, or map,

$$\begin{pmatrix} p^{n+1} \\ q^{n+1} \end{pmatrix} = e^{\Delta\tau V_1} \begin{pmatrix} p^n \\ q^n \end{pmatrix} = \mathbf{V}(\lambda_1, \Delta\tau) \begin{pmatrix} p^n \\ q^n \end{pmatrix}, \quad (2.2)$$

$$\begin{pmatrix} p^{n+1} \\ q^{n+1} \end{pmatrix} = e^{\Delta\tau T} \begin{pmatrix} p^n \\ q^n \end{pmatrix} = \mathbf{T}(m, \Delta\tau) \begin{pmatrix} p^n \\ q^n \end{pmatrix}, \quad (2.3)$$

where \mathbf{T} and \mathbf{V} are matrices given by

$$\mathbf{T}(m, \Delta\tau) = \begin{pmatrix} 1 & 0 \\ \Delta\tau/m & 1 \end{pmatrix}, \quad (2.4)$$

$$\mathbf{V}(\lambda, \Delta\tau) = \begin{pmatrix} 1 & -\Delta\tau\lambda \\ 0 & 1 \end{pmatrix}. \quad (2.5)$$

The Jacobian of the transformation defined by

$$M = \frac{\partial(p^{n+1}, q^{n+1})}{\partial(p^n, q^n)} \quad (2.6)$$

satisfies the defining symplectic condition

$$M^T J M = J, \quad \text{with} \quad J = \begin{pmatrix} 0 & -1 \\ 1 & 0 \end{pmatrix}, \quad (2.7)$$

ensuring that $\det M^T \det M = 1$. For a sequence of symplectic maps, by the chain-rule, the Jacobian multiplies

$$\frac{\partial(p_n, q_n)}{\partial(p_0, q_0)} = \frac{\partial(p_n, q_n)}{\partial(p_{n-1}, q_{n-1})} \cdots \frac{\partial(p_2, q_2)}{\partial(p_1, q_1)} \frac{\partial(p_1, q_1)}{\partial(p_0, q_0)}. \quad (2.8)$$

Regarding (2.2,2.3) as numerical algorithms, the Jacobian matrix is just the error amplification matrix. However, only in the present case of linear maps (2.2,2.3) is the Jacobian the same as the transformation matrix itself.

The error amplification matrix corresponding to the symplectic Euler MTS algorithm

$$\mathbf{e}^{\Delta t(T+V_1+V_2)} = \left[\mathbf{e}^{\Delta\tau T} \mathbf{e}^{\Delta\tau V_1} \right]^k \mathbf{e}^{\Delta t V_2} + O(\Delta t^2) \quad (2.9)$$

is therefore (corresponding to Barth and Schlick's \mathbf{A}_I),

$$\mathbf{e}_E = \left[\mathbf{T}(m, \frac{\Delta t}{k}) \mathbf{V}(\lambda_1, \frac{\Delta t}{k}) \right]^k \mathbf{V}(\lambda_2, \Delta t). \quad (2.10)$$

The symplectic matrices \mathbf{T} and \mathbf{V} as defined by (2.4) and (2.5), can also be expressed as exponentials of traceless matrices:

$$\mathbf{T}(m, \Delta\tau) = \exp \left[\Delta\tau \begin{pmatrix} 0 & 0 \\ 1/m & 0 \end{pmatrix} \right], \quad (2.11)$$

$$\mathbf{V}(\lambda, \Delta\tau) = \exp \left[\Delta\tau \begin{pmatrix} 0 & -\lambda \\ 0 & 0 \end{pmatrix} \right]. \quad (2.12)$$

For large multiple k , the fast force term in (2.10) can be evaluated analytically. Using the exponential forms for \mathbf{T} and \mathbf{V} , and invoking Trotter's theorem,

$$\begin{aligned} \lim_{k \rightarrow \infty} \left(\exp \left[\frac{\Delta t}{k} \begin{pmatrix} 0 & 0 \\ 1/m & 0 \end{pmatrix} \right] \exp \left[\frac{\Delta t}{k} \begin{pmatrix} 0 & -\lambda_1 \\ 0 & 0 \end{pmatrix} \right] \right)^k &= \exp \left[\Delta t \begin{pmatrix} 0 & -\lambda_1 \\ 1/m & 0 \end{pmatrix} \right], \\ &= \begin{pmatrix} \cos(\omega_1 \Delta t) & -m\omega_1 \sin(\omega_1 \Delta t) \\ (m\omega_1)^{-1} \sin(\omega_1 \Delta t) & \cos(\omega_1 \Delta t) \end{pmatrix} \equiv \mathbf{H}(m, \omega_1, \Delta t), \end{aligned} \quad (2.13)$$

where we have defined the fast force angular frequency $\omega_1 = \sqrt{\lambda_1/m}$. Note that one starts with λ_1 and m , but the dynamics of the system is governed by the square root ω_1 . Since ω_1 is a non-analytic function of λ_1 and m , it can only be extracted in the limit of $k \rightarrow \infty$.

The eigenvalues of the fast force error matrix (2.13) is given by

$$e_{1,2} = C \pm \sqrt{C^2 - 1} \quad (2.14)$$

with $C = \cos(x)$ and $x = \omega_1 \Delta t$. The algorithm is marginally stable at all time step Δt with $|e_{1,2}| = 1$, but closest to being unstable at $x = n\pi$, where the two eigenvalues are degenerate, purely real, and equal to ± 1 .

The error matrix corresponding to Euler MTS algorithm (2.10) is therefore

$$\mathbf{e}_E = \mathbf{H}(m, \omega_1, \Delta t) \mathbf{V}(\lambda_2, \Delta t). \quad (2.15)$$

The eigenvalues are still given by (2.14), but now with C altered to

$$C = \cos(x) - \frac{1}{2}\alpha x \sin(x), \quad (2.16)$$

$$= A(x) \cos(x + \delta(x)), \quad (2.17)$$

with $\alpha = \lambda_2/\lambda_1$, amplitude

$$A(x) = \sqrt{1 + (\alpha x/2)^2}, \quad (2.18)$$

and phase shift $\delta(x) = \tan^{-1}(\alpha x/2)$. The two C-functions, together with the amplitude functions $\pm A(x)$, are plotted in Fig.1. The Euler MTS algorithm is unstable whenever $|C(x)| > 1$. As shown in Fig.1, the effect of λ_2 , no matter how small, is to destabilize marginally stable points of the fast force λ_1 at $x = n\pi$ into a finite band. The first band at $x = \pi$, is the half period barrier. The bands are very narrow if $\lambda_2 \ll \lambda_1$. Within these instability bands, the extremes of the eigenvalues at $x + \delta(x) = n\pi$, when $C = \pm A(x)$, are given by (2.14),

$$e(x) = \pm \left(\alpha x/2 + \sqrt{1 + (\alpha x/2)^2} \right). \quad (2.19)$$

This is the linearly growing envelope of eigenvalues observed numerically by Barth and Schlick¹⁸. Since the eigenvalue departs from unity linearly as a function of x , we can characterize this instability as first order in x . This is the most important characterization of MTS algorithms and is plotted in Fig. 2. As one can see, as long as α is not zero, the departure from unity will be significant at $x = \pi$, which explains the persistence of the half period barrier. We emphasize that $e(x)$ only gives the correct eigenvalues at $x + \delta(x) = n\pi$, when $C = \pm A(x)$. For $\alpha \ll 1$, this means that $e(x)$ is only correct at $x \approx n\pi$. For other values of x , $e(x)$ is not the correct eigenvalue and the algorithm is actually stable.

The error matrix for the second order Verlet-like MTS algorithm,

$$\mathbf{e}_V = \mathbf{V}(\lambda_2, \frac{1}{2}\Delta t) \mathbf{H}(m, \omega_1, \Delta t) \mathbf{V}(\lambda_2, \frac{1}{2}\Delta t) \quad (2.20)$$

has the same C-function (2.16) and therefore the identical first order instability problem. This is a surprise. As we will see later in Section IV, increasing the order of *static* MTS algorithms does little to increase its stability.

III. RESTORING STABILITY VIA DYNAMICAL MTS

The MTS algorithm in the last section splits the Hamiltonian as

$$H(p, q) = \left(\frac{p^2}{2m} + \frac{1}{2}\lambda_1 q^2 \right) + \frac{1}{2}\lambda_2 q^2, \quad (3.1)$$

where the parenthesis describes the full dynamics of spring λ_1 . This leaves λ_2 as only a static force with no direct role in changing the particle's position. We shall refer to this as *static* multiple-timestepping. This is not an equitable splitting, nor the only one possible. The Hamiltonian can alternatively be splitted as

$$H(p, q) = \left(\frac{p^2}{2m_1} + \frac{1}{2}\lambda_1 q^2 \right) + \left(\frac{p^2}{2m_2} + \frac{1}{2}\lambda_2 q^2 \right), \quad (3.2)$$

with the constraint

$$\frac{1}{m_1} + \frac{1}{m_2} = \frac{1}{m}. \quad (3.3)$$

Now both springs are fully dynamical and we can use the freedom in the choice of m_1 and m_2 to maximize stability. We shall refer to this as *dynamic* multiple-timestepping. The Euler splitting algorithm of (3.2) in operator form is

$$\mathbf{e}^{\Delta t(T_1+V_1+T_2+V_2)} \approx \mathbf{e}^{\Delta t(T_1+V_1)} \mathbf{e}^{\Delta t(T_2+V_2)}. \quad (3.4)$$

Consider first when both are evaluated exactly as in (2.13), then the error matrix is

$$\mathbf{e}_{DE} = \mathbf{H}(m_1, \Omega_1, \Delta t) \mathbf{H}(m_2, \Omega_2, \Delta t), \quad (3.5)$$

with

$$\Omega_1 = \sqrt{\frac{\lambda_1}{m_1}} \quad \text{and} \quad \Omega_2 = \sqrt{\frac{\lambda_2}{m_2}}. \quad (3.6)$$

The corresponding C-function is

$$C = \cos((\Omega_1 + \Omega_2)\Delta t) - \frac{(m_1\Omega_1 - m_2\Omega_2)^2}{2m_1\Omega_1 m_2\Omega_2} \sin(\Omega_1\Delta t) \sin(\Omega_2\Delta t). \quad (3.7)$$

The destabilizing sine function term can be eliminated by choosing

$$m_1\Omega_1 = m_2\Omega_2 \quad \rightarrow \quad m_1\lambda_1 = m_2\lambda_2. \quad (3.8)$$

Thus stability can be fully restored in this splitting with the choice of

$$\frac{1}{m_1} = \frac{\lambda_1}{\lambda_1 + \lambda_2} \frac{1}{m} \quad \text{and} \quad \frac{1}{m_2} = \frac{\lambda_2}{\lambda_1 + \lambda_2} \frac{1}{m}. \quad (3.9)$$

For this choice of m_1 and m_2 , we observe that

$$\Omega_1 = \frac{\lambda_1}{\lambda_1 + \lambda_2} \Omega \quad \text{and} \quad \Omega_2 = \frac{\lambda_2}{\lambda_1 + \lambda_2} \Omega \quad (3.10)$$

where

$$\Omega = \sqrt{\frac{\lambda_1 + \lambda_2}{m}} \quad (3.11)$$

is the exact angular frequency of the system. This means, however that

$$\Omega = \Omega_1 + \Omega_2, \quad (3.12)$$

i.e., the choice of m_1 and m_2 which restores stability also linearizes the spectrum. To compare with the static case, we also note that

$$\Omega_1 = \sqrt{\frac{\lambda_1}{\lambda_1 + \lambda_2} \frac{\lambda_1}{m}} = \frac{\omega_1}{\sqrt{1 + \alpha}} \quad (3.13)$$

and

$$\Omega_2 = \alpha \Omega_1. \quad (3.14)$$

For MTS algorithms, we do not want to evaluate the second spring force exactly, but only sparingly. Thus we further approximate (3.4) by

$$e^{\Delta t(T_1 + V_1 + T_2 + V_2)} \approx e^{\Delta t(T_1 + V_1)} e^{\Delta t T_2} e^{\Delta t V_2}. \quad (3.15)$$

This is the dynamical Euler MTS algorithm with error matrix

$$\mathbf{e}_{DE} = \mathbf{H}(m_1, \Omega_1, \Delta t) \mathbf{T}(m_2, \Delta t) \mathbf{V}(\lambda_2, \Delta t). \quad (3.16)$$

The resulting C-function is

$$C = \cos(x')(1 - \frac{1}{2}(\alpha x')^2) - \alpha x' \sin(x'), \quad (3.17)$$

where

$$x' = \Omega_1 \Delta t = x / \sqrt{1 + \alpha} \quad \text{and} \quad \alpha x' = \Omega_2 \Delta t. \quad (3.18)$$

This C-function is $\cos(\Omega_1\Delta t + \Omega_2\Delta t)$ correct to second order in $\Omega_2\Delta t$. The corresponding amplitude and eigenvalue functions are

$$A(x') = \sqrt{1 + (\alpha x')^4/4}, \quad (3.19)$$

$$e(x') = \pm \left[(\alpha x')^2/2 + \sqrt{1 + (\alpha x')^4/4} \right]. \quad (3.20)$$

Thus by allowing λ_2 to be dynamical, the same effort in force evaluation improves the instability to second order. This is shown in Fig.2. However, one can do even better. By (3.5), the algorithm's stability will continue to improve with improvements in solving λ_2 's dynamics. With still only one slow force evaluation, one can solve λ_2 's dynamic to second order with error matrix

$$\mathbf{e}_{DE2} = \mathbf{H}(m_1, \Omega_1, \Delta t) \mathbf{T}(m_2, \frac{1}{2}\Delta t) \mathbf{V}(\lambda_2, \Delta t) \mathbf{T}(m_2, \frac{1}{2}\Delta t), \quad (3.21)$$

C-function

$$C = \cos(x') \left(1 - \frac{1}{2}(\alpha x')^2\right) - \alpha x' \left(1 - \frac{1}{8}(\alpha x')^2\right) \sin(x'), \quad (3.22)$$

amplitude

$$A(x') = \sqrt{1 + (\alpha x'/2)^6}, \quad (3.23)$$

eigenvalue

$$e(x') = \pm \left[(\alpha x'/2)^3 + \sqrt{1 + (\alpha x'/2)^6} \right], \quad (3.24)$$

and improve stability to third order! In sharp contrast to the static case, where the use of a second order algorithm for the slow force yielded no improvement in stability, the improvement here is dramatic. As shown in Fig.2, even for α as large as $1/20$, this second order algorithm is basically stable at $x = \pi$.

If one is willing to evaluate the slow force more than once, further systematic improvements are possible. The second spring's motion can be solve to fourth order using forward symplectic algorithm $4A^{9,10}$:

$$\mathbf{e}^{\Delta t(T_2+V_2)} = \mathbf{e}^{\frac{1}{2}\Delta t V_2} \mathbf{e}^{\frac{1}{2}\Delta t T_2} \mathbf{e}^{\frac{2}{3}\Delta t \tilde{V}_2} \mathbf{e}^{\frac{1}{2}\Delta t T_2} \mathbf{e}^{\frac{1}{6}\Delta t V_2} + O(\Delta t)^5. \quad (3.25)$$

Here $\tilde{V}_2 = V_2 + \frac{1}{48}\Delta t^2[V_2, [T_2, V_2]]$. The double commutator modifies the original spring constant λ_2 to

$$\tilde{\lambda}_2 = \lambda_2 \left(1 - \frac{1}{24} \frac{\lambda_2}{m_2} \Delta t^2\right) = \lambda_2 \left(1 - \frac{1}{24}(\alpha x')^2\right). \quad (3.26)$$

The resulting error matrix is

$$\mathbf{e}_{4A} = \mathbf{H}(m_1, \Omega_1, \Delta t) \mathbf{V}(\lambda_2, \frac{1}{6}\Delta t) \mathbf{T}(m_2, \frac{1}{2}\Delta t) \mathbf{V}(\tilde{\lambda}_2, \frac{2}{3}\Delta t) \mathbf{T}(m_2, \frac{1}{2}\Delta t) \mathbf{V}(\lambda_2, \frac{1}{6}\Delta t), \quad (3.27)$$

with C-function

$$\begin{aligned} C = & \cos(x') \left[1 - \frac{1}{2}(\alpha x')^2 + \frac{1}{24}(\alpha x')^4 - \frac{1}{864}(\alpha x')^6 \right] \\ & - \left[\alpha x' - \frac{1}{6}(\alpha x')^3 + \frac{7}{864}(\alpha x')^5 - \frac{1}{10368}(\alpha x')^7 \right] \sin(x'), \end{aligned} \quad (3.28)$$

amplitude

$$A(x') = \sqrt{1 + \frac{1}{36}(\alpha x'/2)^{10} - \frac{2}{3^7}(\alpha x'/2)^{12} + \frac{1}{3^8}(\alpha x'/2)^{14}}, \quad (3.29)$$

and eigenvalue function,

$$e(x') = \pm \left[\sqrt{A^2(x') - 1} + A(x') \right]. \quad (3.30)$$

The instability is now pushed back to fifth order in x . Fig. 2 shows that even for α as large as $1/20$, this algorithm is now basically stable out to $x \approx 6\pi$. For $\alpha = 1/400$, as considered by Barth and Schlick, this algorithm has $e \leq 1.00001$ at $x \approx 50\pi$. There is no doubt that one has overcome the half-period barrier at $x = \pi$.

IV. STABILITY EXPLAINED

The poor stability of static multiple-timestepping can be traced to the non-analytic character the spectrum. The system's exact angular frequency is

$$\Omega = \sqrt{\frac{\lambda_1 + \lambda_2}{m}} = \sqrt{\omega_1^2 + \omega_2^2} = \omega_1 \sqrt{1 + \alpha}, \quad (4.1)$$

with exact C-function

$$C = \cos(\Omega \Delta t). \quad (4.2)$$

In terms of $x = \omega_1 \Delta t = \sqrt{\lambda_1/m} \Delta t$ and $\alpha = \lambda_2/\lambda_1$, this function is non-analytic in α ,

$$C = \cos(x\sqrt{1 + \alpha}). \quad (4.3)$$

When expanded in terms of α , it has the form

$$C = \cos(x) - \frac{1}{2}x \sin(x)\alpha + \left[\frac{1}{8}x \sin(x) - \frac{1}{8}x^2 \cos(x) \right] \alpha^2 + \dots \quad (4.4)$$

The first order term is precisely the first order result (2.16). If one were able to reproduce this expansion, one could in principle systematically restore stability. Unfortunately one cannot; when regarding λ_2 as static, one must expand in powers of $\mathbf{V}(\lambda_2, \Delta t) \propto \lambda_2 \Delta t \propto \alpha x$, and can never reproduce the term $\propto x\alpha^2$ in (4.4) in any finite order. Worse, second and fourth order algorithms do not even reproduce the $(x\alpha)^2$ term with the correct coefficient.

By contrast, in dynamical multiple-timestepping, one has,

$$\Omega = \Omega_1 + \Omega_2, \quad (4.5)$$

and the spectrum is linear in Ω_2 . The corresponding C-function

$$C = \cos(\Omega_1 \Delta t + \Omega_2 \Delta t) = \cos(x' + \alpha x'), \quad (4.6)$$

as shown in the last section, can be systematically reproduced order by order in $(\alpha x')$. Thus dynamical multiple-timestepping linearizes the spectrum and can overcome the half period barrier by going to higher order.

V. GENERALIZATION TO MANY FORCES

For more than two forces, the generalization is easy. Again, using the harmonic oscillator as an illustration, the “ N -forces” case of

$$H(p, q) = \frac{p^2}{2m} + \frac{1}{2} \sum_{i=1}^N \lambda_i q^2, \quad (5.1)$$

can be dynamically splitted as

$$H(p, q) = \sum_{i=1}^N \left(\frac{p^2}{2m_i} + \frac{1}{2} \lambda_i q^2 \right), \quad (5.2)$$

with the primary constraint

$$\sum_{i=1}^N \frac{1}{m_i} = \frac{1}{m}. \quad (5.3)$$

and the pair-wise stability conditions, $i \neq j$,

$$m_i \lambda_i = m_j \lambda_j. \quad (5.4)$$

Both can be easily satisfied by the following generalization of (3.9),

$$\frac{1}{m_i} = \frac{\lambda_i}{\sum_{j=1}^N \lambda_j} \frac{1}{m} = \left(\frac{\omega_i}{\Omega} \right)^2 \frac{1}{m}. \quad (5.5)$$

Thus the inverse of the dynamical mass should be chosen in proportional to the strength of the force, or the square of its angular frequency.

VI. CONCLUSIONS

In this work, we have given a detailed analysis of Barth and Schlick’s model of MTS instability¹⁸. We show that the instability of static MTS algorithms can ultimately be traced to the non-analytic character of the underlying spectrum. Static MTS algorithms are simply very poor starting points for solving such a spectrum, even if one were to modify or average over the slow force¹⁹. By contrast, dynamic MTS algorithms linearize the spectrum, render it analytic, and can improve stability systematically order by order. The use of Langevin dynamics to damp out the instability²⁰ simply masks the true dynamics of the system without fundamentally solving the instability problem.

Realistic biomolecular simulations are too complicated for a detailed stability analysis as in the harmonic oscillator case. Nevertheless, the harmonic oscillator captures the essence of its fast vibrating modes. Thus the insight of dynamic multiple-timestepping can be applied easily. The key idea is to decompose

$$\frac{1}{m} = \frac{1}{m_1} + \frac{1}{m_2} \quad (6.1)$$

and update particles affected by the slow force dynamically with mass m_2 . In the harmonic oscillator case, $1/m_1$ and $1/m_2$ are to be determined in proportional to the strength, or the square of the frequency, of the force. For realistic simulations, one can simply determine the optimal m_2 by trial-and-error subject to the constraint (6.1).

Acknowledgments

This work was supported, in part, by the National Science Foundation grants No. PHY-0100839 and DMS-0310580.

-
- ¹ H. Yoshida, *Celest. Mech. Dyn. Astron.* **56**, 27 (1993).
² P. J. Channell and F. R. Neri, An introduction to symplectic integrators, in *Integration Algorithms and Classical mechanics* (Toronto, ON, 1996), Fields Inst. Commun., 10, Amer. Math. Soc., Providence, RI, P.45.
³ R. I. McLachlan and G. R. W. Quispel, *Acta Numerica*, **11**, 241 (2002).
⁴ E. Forest and R. D. Ruth, *Physica D* **43**, 105 (1990).
⁵ R. I. McLachlan and P. Atela, *Nonlinearity*, **5**, 542 (1991).
⁶ R. I. McLachlan, *SIAM J. Sci. Comput.* **16**, 151 (1995).
⁷ P. V. Koseleff, in *Integration algorithms and classical mechanics*, Fields Inst. Commun., 10, Amer. Math. Soc., Providence, RI, P.103, (1996).
⁸ I. P. Omelyan, I. M. Mryglod and R. Folk, *Phys. Rev.* **E66**, 026701 (2002).
⁹ Siu A. Chin, *Phys. Lett.* **A226**, 344 (1997).
¹⁰ Siu A. Chin, and C. R. Chin, “Forward Symplectic Integrators for Solving Gravitational Few-Body Problems”, arXiv, astro-ph/0304223.
¹¹ H. Grubmüller, H. Heller, A. Windemüth, and K. Schülten, *Mol. Simul.* **6**, 121 (1991).
¹² M. Tuckerman, B. J. Berne, and G. J. Martyna, *J. Chem. Phys.* **97**, 1990 (1992).
¹³ R. Zhou and B. J. Berne, *J. Chem. Phys.* **103**, 9444 (1995).
¹⁴ M. Watanabe and M. Karplus, *J. Phys. Chem.* **99**, 5680 (1995).
¹⁵ J.J. Biesiadecki and R.D. Skeel, *J. Comp. Phys.* **109**, 318 (1993).
¹⁶ M. Mandziuk and T. Schlick, *Chem. Phys. Lett.* **237**, 525 (1995).
¹⁷ T. Schlick, M. Mandziuk, R. D. Skeel, and K. Srinivas, *J. Comput. Phys.* **139**,1 (1998).
¹⁸ E. Barth and T. Schlick, *J. Chem. Phys.* **109**, 1633 (1998).
¹⁹ J. A. Lzaguirre, S. Reich, R. D. Skeel, *J. Chem. Phys.* **110**, 9853 (1999).
²⁰ E. Barth and T. Schlick, *J. Chem. Phys.* **109**, 1617 (1998).

Figures

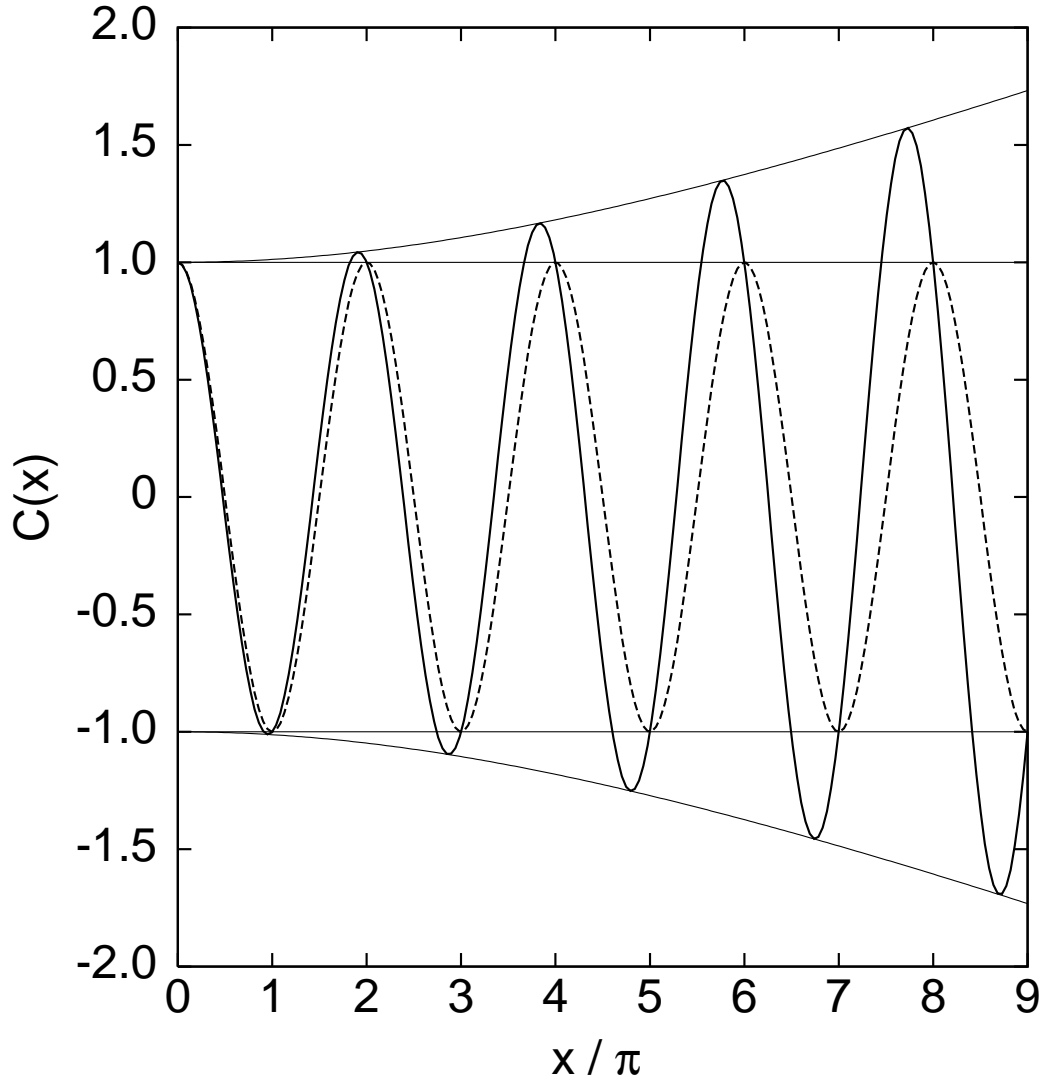


FIG. 1: The fundamental C-function for determining the stability of Multiple-Timestepping (MTS) algorithms. The dashed line gives the stable C-function for the fast force alone, $C(x) = \cos(x)$ where $x = \omega_1 \Delta t$, and ω_1 is the vibrational angular frequency of the fast force. The solid lines give the C-function for the static Euler MTS algorithm, Eq.(2.16). To make the unstable regions visible, a large value of $\alpha = \lambda_2/\lambda_1 = 1/10$ is used, where λ_1 and λ_2 are the force constant of the fast and slow force respectively. The algorithm is unstable whenever $|C(x)| > 1$. The most unstable point in each unstable band near $x \approx n\pi$ touches the amplitude envelope $\pm A(x)$, Eq.(2.18).

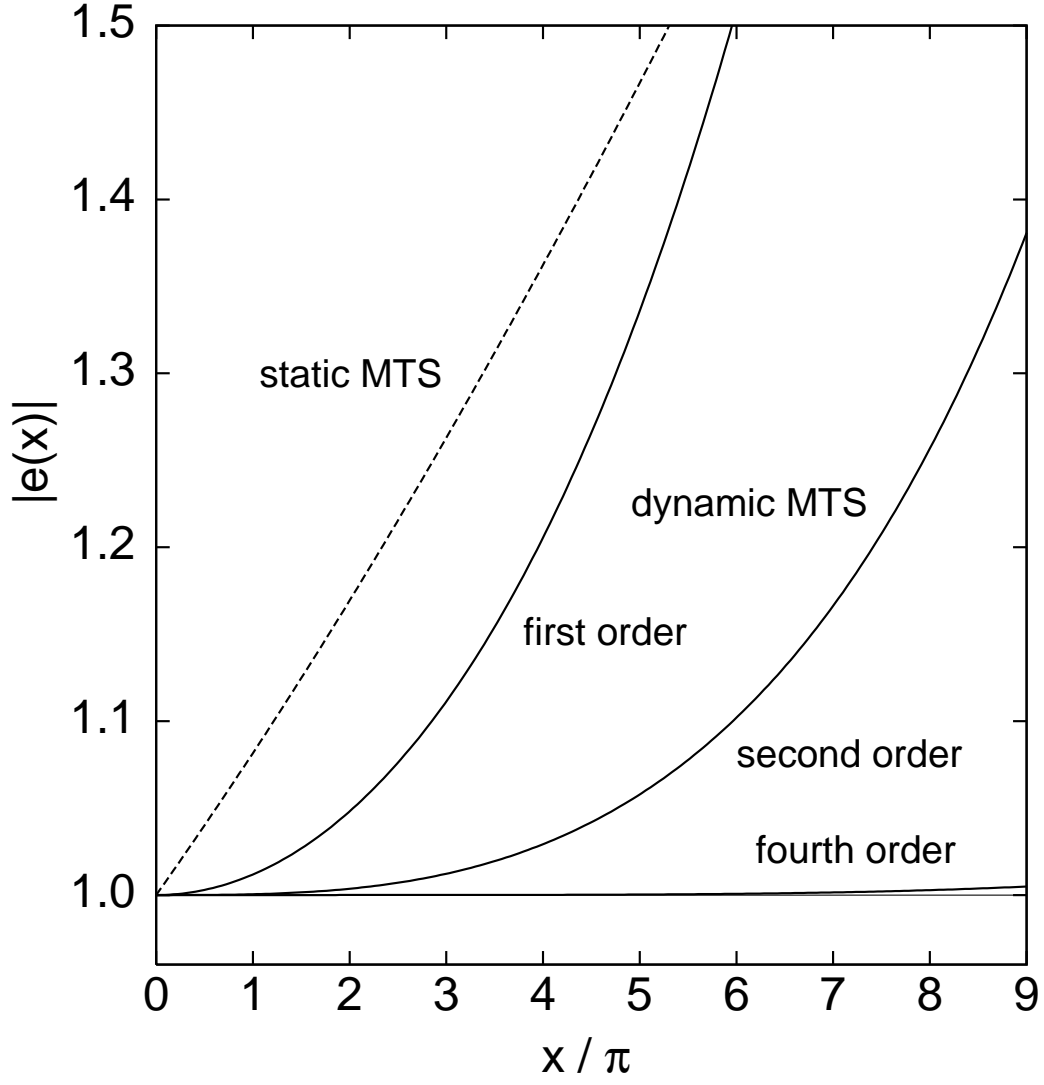


FIG. 2: The magnitude of the error matrix's eigenvalue for various MTS algorithms. The dashed line is the static Euler MTS algorithm. The three solid lines are the three dynamic MTS algorithms described in the text. The algorithm is unstable whenever $|e(x)| > 1$, however, in this graph, only values at $x + \delta(x) = n\pi$ are true eigenvalues. See text for details. A large value of $\alpha = 1/20$ is used to make the fourth order dynamic MTS result visible.